Creep and fracture behaviors of an advanced heat resistant austenitic stainless steel for A-USC power plant

Guocai Chai[1,2*] Patrik Kjellström[1] and Magnus Boström[1]

1 Strategy Research, Sandvik Materials Technology, 811 81 Sandviken, Sweden
2 Engneering Materials, Linköping University, 581 83 Linköping, Sweden
* Corresponding author: guocai.chai@sandvik.com

Abstract Creep and fracture behaviors in a newly developed austenitic stainless steel grade UNS S31035 (Sandvik Sanicro® 25) for use in A-USC power plant have been investigated. This new grade shows very good resistances to steam oxidation and hot corrosion, and higher creep rupture strength than other austenitic stainless steels available today. This makes it an interesting alternative for super-heaters and reheaters in future high-efficient coal fired boilers. This paper will mainly focus on the study of the creep and fracture behaviors of the material at temperatures from 600°C to 750°C by using SEM and TEM. The creep and fracture mechanisms at different temperature and loading conditions have been identified. The interactions between dislocations and precipitates and their contribution to the creep rupture strength have been discussed. In this paper, free temperature model has been used to evaluate the long-term creep behavior of the grade. A creep rupture strength near 100MPa at 700°C for 100 000h has been predicted.

Keywords Heat resistant austenitic stainless steel, Superheater, A-USC, Creep, Fracture

1. Introduction

The demand for electric power is continuously increasing around the world. Meanwhile the consciousness of the environmental impact from human action is growing. Although combustion processes generate carbon dioxide, coal-fired thermal power generation is still one of the most important methods in the medium to long-term future to satisfy this demand, since coal is available at a competitive price and often is the single domestic energy source [1]. However, the biggest challenge facing coal-fired power plants is to improve their energy efficiency. This can be accomplished by increasing the maximum steam temperature and the steam pressure. Conventionally, the heat efficiency of coal-fired power plants has stayed at around 41% in the super critical (SC) condition with a temperature of 550°C and pressure of 24.1MPa. In order to attain a power generating efficiency of about 43%, ultra super critical (USC) conditions with a steam temperature at about 600°C should be reached. By increasing the temperature up to 700°C (A-USC condition) and pressure of above 300 bars, a power plant efficiency of higher than 50% can be reached and CO_2 emission can be reduced by about 45% comparing with that of SC condition [2]. However, the steam data in practice will be limited by the material properties of the boiler tubes, especially tensile strength at elevated temperatures and creep strength combined with corrosion resistance.

A new austenitic stainless steel grade, UNS S31035 (Sandvik Sanicro 25), has recently been developed for the purpose of A-USC [3] in collaboration with a number of different industrial partners within the Thermie-project in Europe, intended for use in super-heaters and reheaters in advanced ultra-supercritical boilers at temperatures up to 700°C. They have been test-installed in different boilers in Europe and have run for more than five years, and are still in very good conditions [4]. In this paper the creep and fracture behaviors of this new grade are discussed.

2. Material and experimental

Since austenitic stainless steel grade, UNS S31035, was aimed for use in super-heaters and reheaters with metal temperatures up to 700°C, the design principles for this alloy were to achieve a stable microstructure, high strength by precipitation strengthening with stable nano precipitates and solution hardening, high corrosion resistance with high Cr content. Ni and N that can suppress the formation of sigma phase were added to reach sufficient structural stability and good fabricability. The chemical composition is shown in Table 1.

Table 1 Nominal composition of austenitic stainless steel grade, UNS S31035 (wt%)

C_{max}	Si	Mn	Cr	Ni	W	Co	Cu	Nb	N	Fe
0.1	0.2	0.5	22.5	25	3.6	1.5	3.0	0.5	0.23	Bal.

Figure 1 shows some fine precipitates observed in this newly developed austenitic stainless steel grade, UNS S31035 that can contribute to the improvement of the creep strength. Both intra- and intergranular $M_{23}C_6$ precipitates can be observed (Fig. 1a). In the grain boundaries, they have a $<100>_{\gamma}$ // $<100>_{M23C6}$ coherent relationship to the austenite matrix. Laves phase was observed both randomly within the grains but also ordered on what appears to be former twin boundaries (Fig. 1b). Both coherent Laves phase precipitates with a $[100]_{Laves}$ // $[100]_{\gamma}$ orientation relationship, and incoherent Laves phase precipitates were observed. In the aged material the Laves phase are needle shaped but rather small. In the creep tested materials, these particles are fine and isometric. Copper rich nanoparticles can also be observed. They are round with a size up to 50 nm (Fig. 1c). In this material, a dense distribution of about 10 nm large precipitates was observed (Fig. 1d). Due to the limitation of the TEM, these particles could not be identified, but they are probably MX carbides or carbonitrides. Similar particles have been identified in other analyses. These particles were rather stable [5].

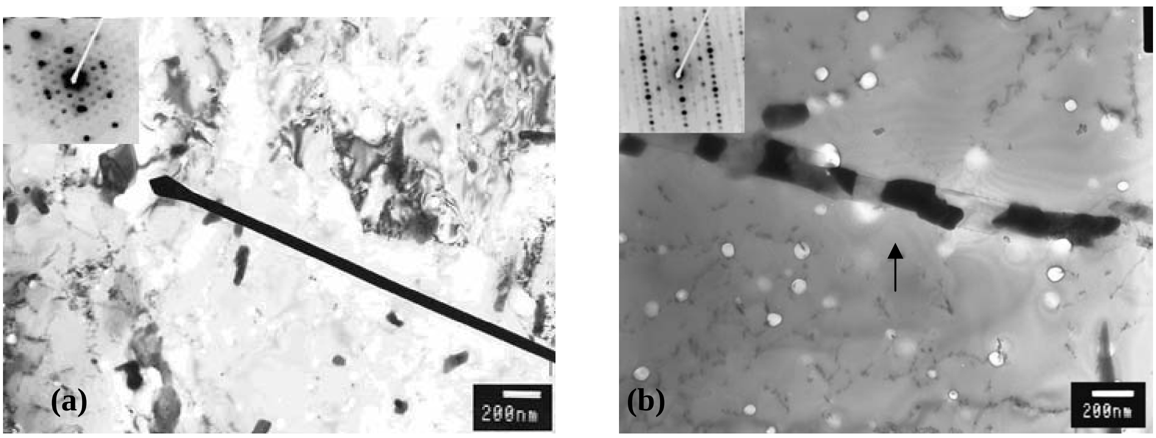

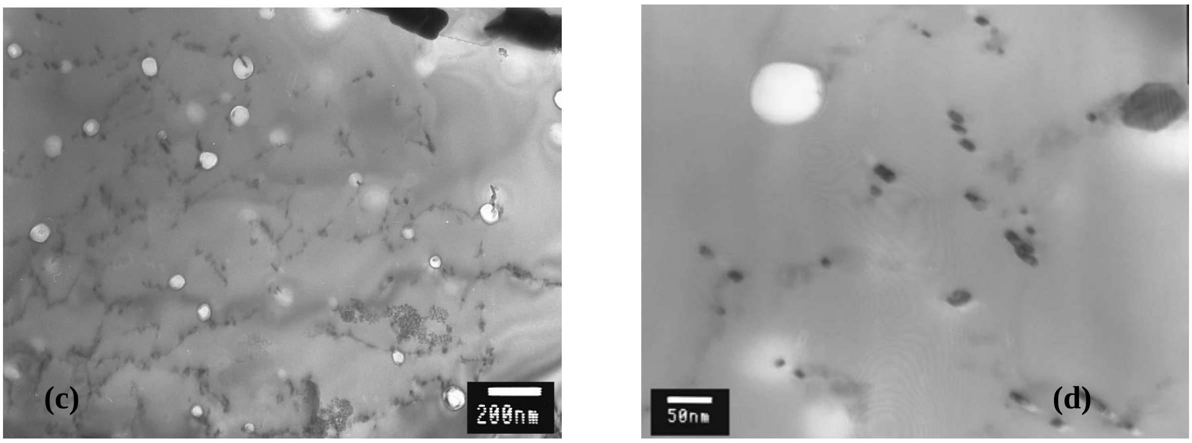

Figure 1. Fine precipitates that contribute to the creep strength of austenitic stainless steel grade, UNS S31035, (a) $M_{23}C_6$, 700°C for 1000 hours, (b) Laves phase, 700°C for 30 000 hours, (c) Copper-rich phase, 700°C for 30 000 hours, (d) Nanoparticles, 700°C for 30 000 hours.

The creep testing on UNS S31035 was performed from 550°C to 800°C. Both stress-rupture testing and creep-strain testing were done. The stress-rupture testing was performed in Escher Wyss (EW) creep testing machines. In these machines multiple samples can be tested simultaneously. The samples (Fig. 2) are mounted in the EW boxes. The tube in which the samples are located is then inserted into the furnace. The load from the compressed spring is applied after the samples have been heated in the furnace for one hour. The creep-strain testing was performed in Bofors machines. The sample was mounted in sample holders in the tube furnace and connected to thermocouples which can measure the temperature continuously. The strain was measured by two extensometers placed outside the furnace. The strain was logged manually regularly during testing to obtain creep curves.

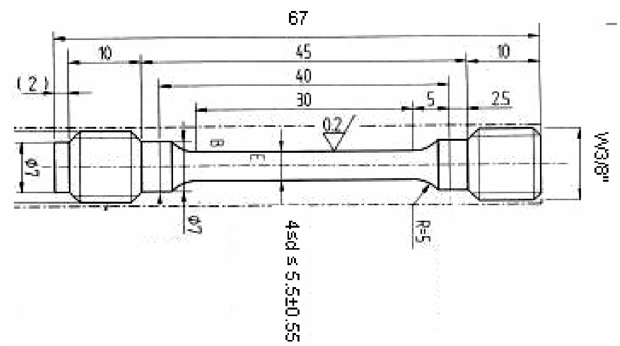

Figure 2. Schematic sample for the creep test.

The microstructure was studied using light optical microscope (LOM), scanning electron microscope (SEM) and transmission electron microscope (TEM). LOM and SEM were used to obtain information on features such as grain size, creep deformation, precipitates and how these changes with time, temperature and stress. TEM was used for phase identification and dislocation structure characterization.

3. Free temperature model

Pressure vessel components are normally designed for a long service time such as 200 000 h. Since creep is a very slow process, creep data for such a time are not available for design. They are therefore calculated by an extrapolation from the creep data of shorter time tests. One recently proposed procedure for extended extrapolation of creep rupture data is the free temperature model that allows for extrapolation by more than a factor of three in time [6, 7]. The procedure is based on a time-temperature parameter (TTP) which has the general mathematical form:

$$P_{TTP} = v(T)\log(t_r) + w(T) \tag{1}$$

where P_{TTP} is the time-temperature parameter, t_r is the time to rupture, and v(T) and w(T) are the functions of temperature. In the proposed procedure these functions are assumed to be polynomials in T. The TTP in Eq. 1 is referred as the free temperature model (FTM). The free temperature model is well suited for austenitic stainless steels where the temperature dependence of the creep rupture curve is non-monotonous [7].

The master curve is expressed by the creep stress as a function of polynomial in the TTP:

$$\log(\sigma) = \sum_{j=0}^{n_P} a_j TTP^j \tag{2}$$

The coefficients a_j are fitted to the creep rupture data and the stress – rupture time relations are derived. The reason for using a polynomial in log (t_r) rather than log (σ) which is the more common approach, is that it has been shown that this improves the accuracy in extended extrapolated values [7]. The extrapolation was performed in a Matlab program. The coefficients to the polynomials are derived by a non-linear least squares fit to the creep data.

To extrapolate the creep rupture data, the polynomials in Eq. 1 were both set to order 3 and the master curve, Eq. 2, was set to a second order polynomial. Figure 3 shows the master curve for the free temperature model of the austenitic stainless steel grade, UNS S31035, which is based on creep data at 550°C, 600°C, 650°C, 700°C and 800°C.

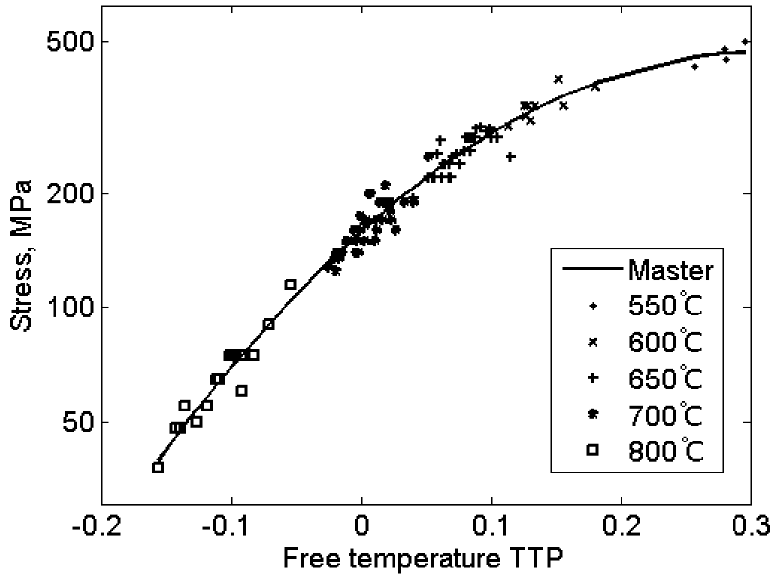

Figure 3 Master curve for austenitic stainless steel grade, UNS S31035, material.

4. Results and discussion
4.1 Creep strength

Up to now, the longest time to rupture from the creep test of this alloy is more than 74 000 h and some samples are still running. Figure 4 shows the results of the creep stress in rupture plots. With linear least squares regression (Larson-Miller relation) to extrapolate the creep rupture data, the predicted 10^5 h creep rupture strength at 700ºC is 104 MPa.

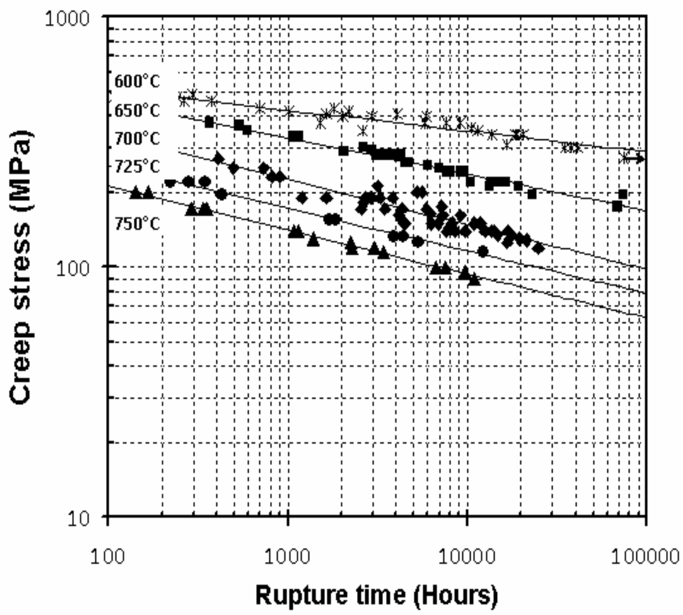

Figure 4 Creep stress versus rupture time of austenitic stainless steel and the linear regressions in the creep data.

The extrapolation was performed three times with rupture data up to 40000 h, 15000 h and 5000 h to verify the stability of the extrapolation. Figure 5a shows the result from the extrapolation. At both 700°C and 650°C the extrapolation overestimates the creep strength of the material when only short time creep data are used. This is common for many parametric methods and it is important that the deviation is not too large. The order of the polynomials and which temperature data sets the model is applied to will also influence the result. These factors are tested until a satisfactory result has been found. The predicted 10^5 h creep rupture strength at 700°C is about 99 MPa.

In Figure 5b, the correlation between the extrapolation and experimental data can be seen. The evaluation satisfies the post evaluation tests (PATs) and other criteria proposed by the European Collaborative Creep Committee (ECCC) [8].

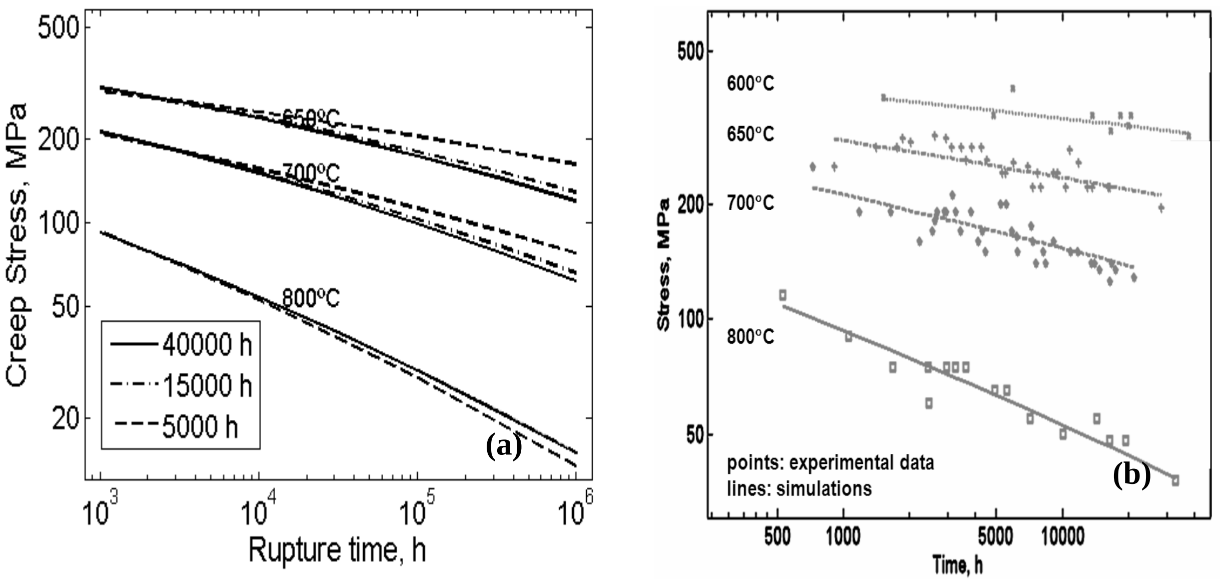

Figure 5 (a). Result from extrapolation with the free temperature model, performed three times with rupture data up to 5000 h, 15000 h and 40000 h, (b). Correlations between the extrapolation with rupture data up to 40000 h and the experimental data.

4.2 Strengthening mechanism

In the temperature range up to 700°C, one of the main creep strengthening mechanisms is the interaction between dislocations and precipitates [9]. Figure 6 shows two examples how interaction between the dislocations and precipitates in austenitic stainless steel grade, UNS S31035, creep specimen tested with 210 MPa at 700°C and with a rupture time of 3153 h. Moving dislocations at the nano-sized particles can be seen. Around the intergranular precipitates, the dislocation density is high which indicates that they function as obstacles for the dislocation movements. This increases the creep strength. Smaller nanoprecipitates such as copper rich particles and MX particles are more effective as obstacles for the dislocation movements. However, they have different mechanisms for dislocation crossing. For the copper rich nanoparticles, dislocations cross the particles mainly by climb / bypass of unit dislocations (Fig. 6a). For the MX nanoparticles, deformation might occur by shearing of partial dislocations. The shadow around the particle in Figure 6b is believed to be dense dislocations. For MX particles, dislocation loops can be observed around the particles (Fig 6c and d).

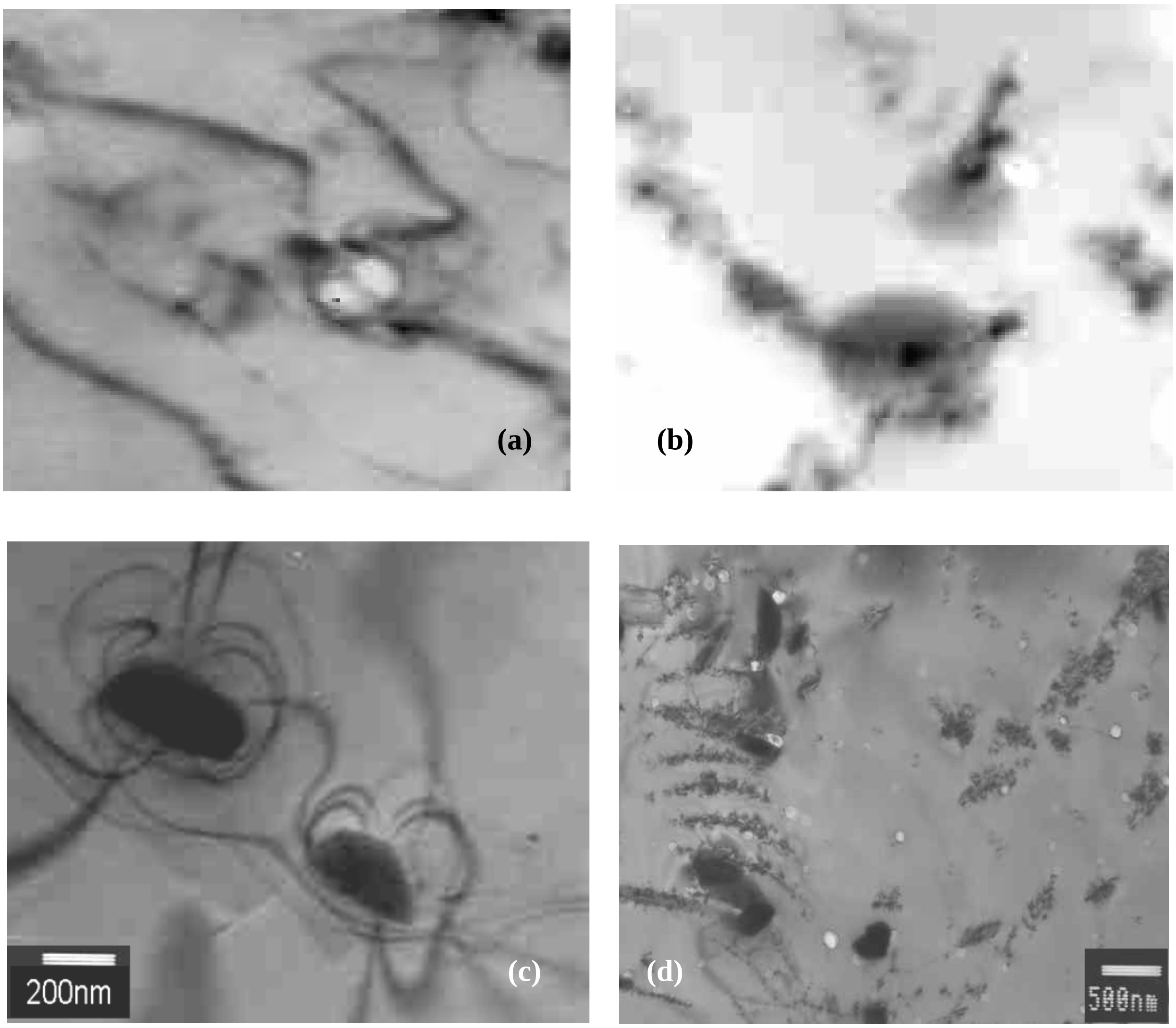

Fig. 6 Dislocation structures, (a). Interaction between dislocations and precipitates, (b). dislocation cloud or cluster near nona Cu-rich particles and MX particles

4.2 Rupture mechanisms

Figure 7 shows an investigation of the fracture modes such as transgranular or intergranular fractures and plastic deformation by creep in UNS S31035 material. A summary of the creep fracture modes are shown in Figure 8.

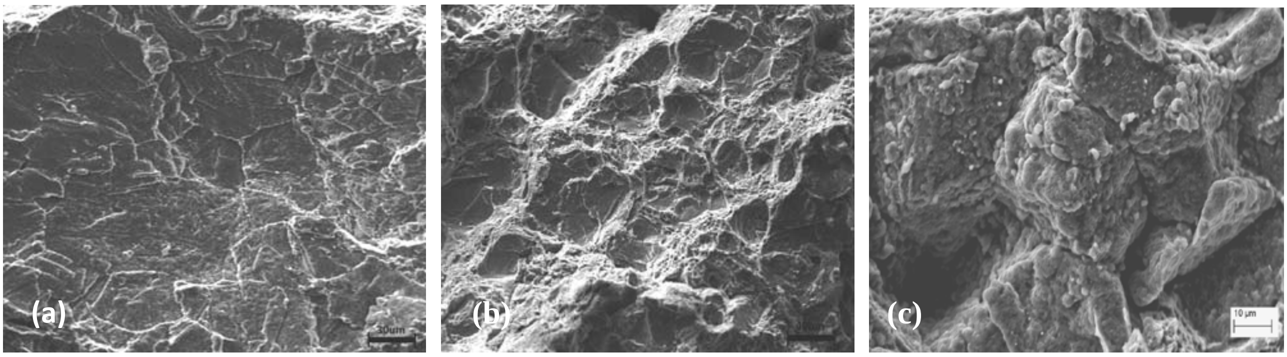

Figure 7 SEM micrograph of creep specimen near the fracture, (a). 700°C/240MPa, 1085h, transgranular cracking, (b). 700°C/210 MPa, 4203h, transgranular and intergranular mixed model, (c). 700°C/150 MPa, 14040 h, intergranular cracking

Plastic deformation and transgranular fracture is the main creep fracture mechanism in UNS S31035 material in the temperature ranges of interest (<700°C). The SEM analysis shows that the crack initiation area was mainly quasi cleavage and then cracks propagated with dimples. At intermediate stresses and temperatures a mixture of inter- and transgranular fracture occurs. The crack initiation often occurs at grain boundaries but propagate through the grains. At relatively low stresses and high temperatures, intergranular fracture could occur. However, plastic deformation can still be observed in these specimens.

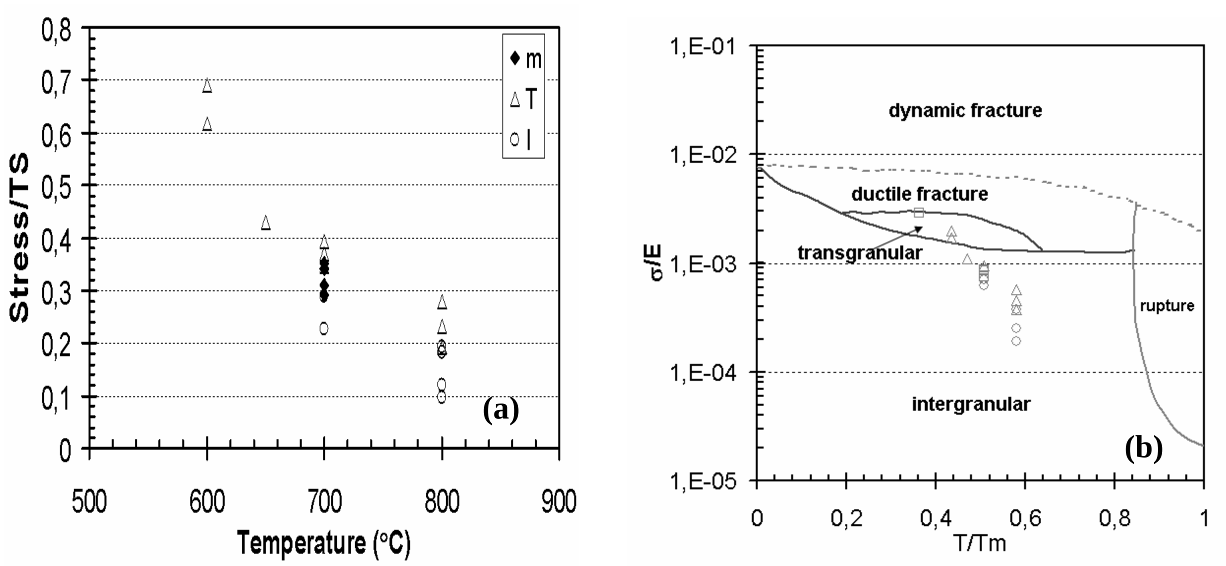

Figure 8 Fracture modes in UNS S31035 at different test conditions.

4. Conclusions

A new austenitic stainless steel grade, UNS S31035 (Sandvik Sanicro 25), has been developed intended for superheater and reheaters for A-USC. Extrapolation from creep data with two methods gives a creep strength of 99 ± 3 MPa at 700°C for 100 000 h, which is higher than that of other austenitic stainless steels available today.

The creep strength is related to intragranular precipitates and nano particles acting as obstacles for dislocation movement.

Plastic deformation and transgranular fracture is the main creep fracture mechanism in the creep test samples of UNS S31035 for high applied stresses, but trend to intergranular fracture with decreasing stresses and increasing temperature.

Acknowledgements

This paper is published by permission of Sandvik Materials Technology.

References

[1] IEA, 2009 energy statistics, http://www.iea.org/stats, (2010-02-25).
[2] R. Blum, R.W. Vanstone and C. Messelier-Gouze, Materials Development for Boilers and Steam Turbines Operating at 700 °C, Proc. 4th Int. Conf. on Adv. in Mater. Technol. for Fossil Power Plant, (2004) 116.
[3] R. Rautio, S. Bruce, Sandvik Sanicro 25, a new material for ultra supercritical coal fired boilers, Proc. 4th Inter Conf. on Adv. in Mater. Technol. for fossil power plants, (2004) 274.
[4] G. Chai, J.O. Nilsson, M. Boström, J. Högberg and U. Forsberg, Advanced Heat Resistant Austenitic Stainless Steels, Proc. of ICAS 2011 (2010) 56.
[5] G. Chai, M. Boström, M. Olaison and U. Forsberg, Creep and LCF behaviors of newly developed advanced heat resistant austenitic stainless steel for A-USC, Procedia Engineering 2012, in press
[6] R. Sandström, Journal of Testing and Evaluation, 31 (2003) 58-66.
[7] R. Sandström and L. Lindé, Precision in the extrapolation of creep rupture data, Journal of Testing and Evaluation Vol. 27, No3 (1999) 203-210.
[8] Generic recommendations and guidance for the assessment of full size creep rupture datasets, ECCC recommendations - volume 5 part in [issue 5], 2008.
[9] J. Högberg, G. Chai, P. Kjellström, M. Boström, U. Forsberg and R. Sandström, (2010), Creep behavior of the newly developed advanced heat resistant austenitic stainless steel grade UNS S31035, PVP2010-25727, Bellevue Washington, USA.